Understanding Phase Stability in Silica/Surfactant Composites through the Study of a Curvature Driven Rectangular Intermediate

Adam F. Gross, Van H. Le, Bradley L. Kirsch, and Sarah H. Tolbert*

Department of Chemistry and Biochemistry, University of California, Los Angeles, Los Angeles, California 90095-1569

Received December 27, 2000. In Final Form: March 13, 2001

Hydrothermal chemistry is used to alter phase stability in ordered silica/surfactant composites. These materials, which are studied using real time X-ray diffraction, display a direct hexagonal-to-lamellar transformation when heated in water. When treated in a pH 11 buffer, however, low angle X-ray diffraction (XRD) reveals an intermediate centered rectangular phase during the phase transformation. By examining the kinetics of this transformation under a range of temperature conditions, we can understand how silica chemistry, interfacial charge density, and surfactant packing interplay to control phase stability. For example, if a lower transformation temperature is used, a hexagonal-to-rectangular-to-lamellar phase progression is observed. Higher transformation temperatures display more complex phase behavior, showing both a direct hexagonal-to-lamellar phase transition and the hexagonal-to-rectangular-to-lamellar transformation occurring at the same time. The observed ordering of phases is consistent with activation energies calculated using the Ozawa method for nonisothermal experiments and the Avrami equation for Arrhenius-based isothermal kinetics. The hexagonal-to-rectangular transformation has an activation energy of 104 ± 7 kJ/mol (Ozawa) while the rectangular-to-lamellar phase transition has an activation energy of 147 ± 7 kJ/mol (Ozawa) or 140 ± 20 kJ/mol (Arrhenius). The unit cell area of the material can also be tracked over the heating ramp to learn more about the transformation. As the material transforms to the rectangular structure, the unit cell area drastically decreases, suggesting that curvature, rather than surfactant volume, drives the rearrangement. The results in this work provide a basis for better understanding the factors that affect phase stability and the relationship between atomic scale silica chemistry and nanoscale order in periodic surfactant templated silicas.

Introduction

The cooperative self-organization of inorganic silica oligomers and organic alkylammonium surfactants can be used to form periodic mesostructures whose phase depends on silica charge density and surfactant packing.[1,2] Hydrothermal treatment modifies the silica charge density and surfactant packing in these materials, which can result in phase transformations.[2,3] While changes in silica charge density are a local phenomenon, changes in surfactant packing occur cooperatively over a larger volume. The connection between these two length scales governs the energetics and kinetics of phase stability in these materials. The atomic scale bonding of the silica, for example, provides a kinetic barrier to the phase transition (framework bonds must be broken for rearrangement). To understand the relationship between the two related length scales, we follow a hexagonal phase silica/surfactant composite as it transforms to a lamellar phase composite under modified hydrothermal conditions. Using a high pH buffer as the hydrothermal solution, we can accelerate silica hydrolysis rates[4] and thus potentially alter the size of the kinetic barrier resulting from the condensed silica network. In addition, we can examine how pH dependent chemistry alters the surfactant ordering and phase stability in these materials.

Changes in reaction kinetics may result in modified transformation temperatures or, more interestingly, transformations to phases other than the expected ones. In these experiments, an intermediate phase between the hexagonal and lamellar phases is observed. The discovery of an intermediate phase is fortuitous because it can provide significant insight into the energetic and mechanistic pathways that connect the initial and final phases. Since the details of a discontinuous solid−solid phase transition mechanism cannot be directly observed, an intermediate phase can be very helpful because it shows the structure of the material between the start and end of the transformation, thus providing more structural information to determine the transformation pathway and mechanism.

Understanding why intermediates form in analogous systems should help us understand how our reaction conditions affect our samples. Multiple intermediate phases have been found in lyotropic liquid crystals that are based on the same alkyl trimethylammonium surfactants as those used in this work.[5−7] In these liquid crystalline materials, a *p*6*mm* hexagonal phase converts to a L_α lamellar phase upon the addition of surfactant. However, an intermediate *cmm* centered rectangular and/or an *Ia*3*d* cubic phase is usually observed at intermediate surfactant concentrations. The centered rectangular phase

* Corresponding author. E-mail: tolbert@chem.ucla.edu.

(1) Kresge, C. T.; Leonowitz, M. E.; Roth, W. J.; Vartuli, J. C.; Beck, J. S. *Nature* **1992**, *359*, 710. Beck, J. S.; Vartuli, J. C.; Roth, W. J.; Leonowicz, M. E.; Kresge, C. T.; Schmitt, K. T.; Chu, C. T.-W.; Olson, D. H.; Sheppard, E. W.; McCullen, S. B.; Higgins, J. B.; Schlenker, J. L. *J. Am. Chem. Soc.* **1992**, *114*, 10834.

(2) Huo, Q.; Margolese, D. I.; Stucky, G. D. *Chem. Mater.* **1996**, *8*, 1147.

(3) Gross, A. F.; Ruiz, E. J.; Tolbert, S. H. *J. Phys. Chem. B* **2000**, *104*, 5448.

(4) Iler, R. K. *The Chemistry of Silica: Solubility, Polymerization, Colloid and Surface Properties, and Biochemistry*; Wiley: New York, 1979.

(5) Henriksson, U.; Blackmore, E. S.; Tiddy, G. J. T.; Söderman, O. *J. Phys. Chem.* **1992**, *96*, 3894.

(6) Blackmore, E. S.; Tiddy, G. D. T. *J. Chem. Soc., Faraday Trans. 2* **1988**, *84*, 1115.

(7) Auvray, X.; Petipas, C.; Anthore, R.; Rico, I.; Lattes, A. *J. Phys. Chem.* **1989**, *93*, 7458.

10.1021/la0018080 CCC: $20.00
Published on Web 05/04/2001

consists of ovoid tubes placed on a centered rectangular lattice; this rectangular lattice is related to the *p*6*mm* hexagonal structure by a distortion along one axis.[8,9,10] Intermediate phases are more commonly observed in liquid crystals than in composite materials because of the fluid nature of liquid crystals. The un-cross-linked nature of liquid crystals allows the surfactant to actively rearrange in multiple configurations to form the most thermodynamically stable structure.

In these liquid crystals, the thermodynamically stable phase is determined by a combination of charge density and surfactant geometry, which together control the interfacial curvature of the material.[6,9,10] A hexagonal phase has high curvature with the surfactant headgroups spaced far apart and the tails packed close together. A lamellar phase has no curvature with equal spacing between the surfactant headgroups and tails. Intermediate phases, such as the *Ia*3*d* cubic or *cmm* centered rectangular phases, have intermediate curvatures that lie between the hexagonal and lamellar structures. Both the surfactant shape and the electrostatic interactions in the solution control this curvature. For example, a higher ionic strength in the aqueous phase of a liquid crystal material screens electrostatic repulsions and therefore lowers the curvature by encouraging the surfactant heads to pack closer together.[8,9] The role of surfactant geometry is seen by varying the alkyl chain length in liquid crystals. Short chain trimethylammonium surfactants form an *Ia*3*d* cubic phase while medium length surfactants form both cubic and *cmm* type intermediate phases. Long chain surfactants generally form only *cmm* centered rectangular phases or other similar phases.[6,11] The tendency for long alkyl chain surfactants to form centered rectangular phases may be rooted in the fact that these longer, more flexible chains can more easily accommodate the mixed curvature which is present in the *cmm* phase but not in the *Ia*3*d* structure. Alternatively, the rectangular phase may let long alkyl chains pack tightly together, thus accommodating surfactant more efficiently.

All phases found in alkyltrimethylammonium surfactant/water liquid crystals have also been synthesized as silica/surfactant composites. This includes the *Ia*3*d* cubic and *cmm* centered rectangular phases as well as the more common *p*6*mm* hexagonal and lamellar structures.[2,12,13] Hexagonal and lamellar composite materials are easily synthesized using simple alkyltrimethylammonium surfactants, but direct synthesis of the cubic and rectangular materials frequently requires a designer surfactant that can be both difficult and time consuming to synthesize.[2,13] While the *Ia*3*d* cubic phase can be formed via a phase transition from the *p*6*mm* hexagonal phase,[12,14,15] neither cubic nor rectangular morphologies have been identified as intermediates during phase transformations, even though they are commonly found in such roles in liquid crystal systems. A plausible explanation for the lack of intermediates is that the silica framework provides a kinetic barrier to transformation that is not present in fluid lyotropic liquid crystals. This barrier prevents the facile formation of intermediate phases.

Understanding how the silica framework and surfactant density are modified during hydrothermal synthesis will also aid in interpreting our results. Recent work has shown that the activation barrier for rearrangement changes with reaction time during synthesis and that the interaction of cosurfactants with the primary surfactant can be used to control how curvature evolves in composite materials.[16−18] Changes in the activation energy for rearrangement were determined by examining whether the composite could swell or rearrange in response to the addition of a cosolvent. The results indicate that a more condensed framework (i.e. longer reaction time) inhibits rearrangement, but that under conditions where the framework is fairly fluid, both increases and decreases in composite curvature can be driven by addition of the appropriate cosurfactant.[16−18] The results clearly indicate that surfactant packing will dominate composite structure when possible but that the rigidity of the silica framework can prevent optimization of the nanoscale architecture on kinetic grounds.

In our experiments, instead of using time to modify the kinetic barrier for rearrangement, we take advantage of the strong dependence of silica chemistry on pH.[4,19] In addition to affecting the bonding within the silica framework, pH can also be used to modify the interaction between the framework and the organic template. The high pH buffer used in these hydrothermal solutions will make the silica surface highly charged, resulting in many $Si-O^-$ sites that can interact electrostatically with the surfactant. This should change the optimal surfactant packing relative to hydrothermal treatment in pure water and should tend to discourage the surfactant loss that occurs upon hydrothermal treatment in pure water. An example of the effect of a high pH solution is illustrated by the material studied in this work: the composite undergoes a transition from a hexagonal structure directly to a layered, lamellar phase under pure water hydrothermal conditions,[2] but if treated in a pH 11 buffer where silica hydrolysis rates are significantly higher, it transforms via a *cmm* rectangular phase intermediate.[4,19] The *cmm* phase requires a higher surfactant concentration than the hexagonal phase in liquid crystals. Analogously, less surfactant should be lost in these high pH experiments compared to those performed in water.

A final important aspect of this work is the demonstration that thermal treatment profiles can be used to control the observed phase of the composites and to learn about the relative kinetic accessibility of the possible reaction pathways. Altering the kinetic barrier to transformation is possible using variable heating profiles because silica polymerization and surfactant density depend on the thermal history of the material.[3] Understanding this interplay can have practical effects for materials synthesis. For example, previous experiments on hexagonal silica/surfactant composites heated in their high pH synthesis solutions show that the composite transforms to both a desired cubic structure and the more common lamellar phase, but the resulting population of these phases depends on the time the material is reacted before heating

(8) Husson, F.; Mustacchi, H.; Luzzati, V. *Acta Crystallogr.* **1960**, *13*, 668.
(9) Hagslätt, H.; Söderman, O.; Jönsson, B. *Liq. Cryst.* **1992**, *12*, 667.
(10) Hagslätt, H.; Söderman, O.; Jönsson, B. *Liq. Cryst.* **1994**, *17*, 157.
(11) Rendall, G.; Tiddy, G. J. T.; Trevethan, M. A. *J. Chem. Soc., Faraday Trans. 1* **1983**, *79*, 637.
(12) Gallis, K. W.; Landry, C. C. *Chem. Mater.* **1997**, *9*, 2035.
(13) Zhao, D.; Huo, Q.; Feng, J.; Kim, J.; Han, Y.; Stucky, G. D. *Chem. Mater.* **1999**, *11*, 2668.
(14) Xu, J.; Luan, Z. H.; He, H. Y.; Zhou, W.-Z.; Kevan, L. *Chem. Mater.* **1998**, *10*, 3690.
(15) Pevzner, S.; Regev, O. *Microporous Mesoporous Mater.* **2000**, *38*, 3:413.
(16) Lindén, M.; Ågren, P.; Karlsson, S.; Bussian, P.; Amenitsch, H. *Langmuir* **2000**, *16*, 5831.
(17) Ågren, P.; Lindén, M.; Rosenholm, J. B.; Blanchard, J.; Schüth, F.; Amenitsch, H. *Langmuir* **2000**, *16*, 8809.
(18) Ågren, P.; Lindén, M.; Rosenholm, J. B.; Schwarzenbacher, R.; Kriechbaum, M.; Amenitsch, H.; Laggner, P.; Blanchard, J.; Schüth, F. *J. Phys. Chem. B* **1999**, *103*, 5943.
(19) Brinker, C. J. *Sol−Gel Science: The Physics And Chemistry Of Sol−Gel Processing*; Academic Press: Boston, 1990.

and how hot it is heated.[12,20,21] The bifurcation of the two phases suggests that the lamellar phase is kinetically favored, but the cubic phase is more energetically stable. A better understanding of intermediate phases and the dependence of these phases on complex reaction pathways is, therefore, not only scientifically beneficial but also practically useful. This knowledge may aid in understanding how to access previously unseen phases and thus further develop novel silica/surfactant composite materials. For example, nonionic block copolymer liquid crystals form a range of phases[22] that have not yet been synthesized in mesopores. The results of this experiment may make choosing appropriate processing conditions to access a desired phase somewhat easier. In addition, a more complete picture of the relationship between chemistry on the atomic length scale and ordering on the nanometer length scale will be developed.

Experimental Section

The silica/surfactant composites used in this work result from the self-organization of a positively charged quaternary ammonium surfactant interacting with reactive silicate oligomers. The surfactant, $CH_3(CH_2)_{19}N(CH_3)_3Br$, was synthesized from $N(CH_3)_3$ and $CH_3(CH_2)_{19}Br$ by established methods.[23] A basic surfactant solution (0.024 M surfactant and 0.235 M NaOH) was mixed with tetraethylorthosilicate (TEOS) to produce a final silica concentration of 0.410 M. The mixture was stirred for 1 h, after which the resulting powder was filtered, washed with water, and dried. The powder was mixed with a pH 11 boric acid buffer (0.250 M H_3BO_3 combined with 0.243 M tetraethylammonium hydroxide) immediately prior to the experiment.

The phase transition was followed using real time X-ray powder diffraction. Data were collected at the Stanford Synchrotron Radiation Laboratory on wiggler beamline 10-2 using an X-ray energy of 9 keV. Samples were prepared by mixing the composite with buffer in a weight-to-weight ratio of 1:20. The resulting slurry was injected into a quartz capillary tube that was sealed with a graphite ferrule under a dynamic 330 psi N_2 back-pressure. The assembly was rocked throughout the experiment in the X-ray beam, which served to mix the sample, increase the uniformity of heating, and average the diffraction pattern.[24] Samples were heated by linearly increasing the temperature or holding the temperature at a constant value using a calibrated Omega PID feedback controlled air stream. The distance between the heat source and the sample was controlled so that it was the same for all samples. The temperature offset between the thermocouple and the sample was calibrated using a 3-point linear correction based on room temperature, the melting point of sulfur (mp = 117 °C), and the melting point of ascorbic acid (mp = 190 °C). The buffer changed from pH 11.0 to pH 10.4 during the course of the experiment.

For nonisothermal (linearly ramped temperature) experiments, data were collected in 30 s acquisitions using a Roper Scientific 1242 × 1152 cooled X-ray CCD detector. Multiple ramp rates of 8.77, 4.40, and 2.22 °C/min were used to examine kinetic effects on the phase transition temperature. In isothermal experiments, the sample was heated to a set temperature using a 2 min ramp, and then held at the set temperature. Data were collected in 20 s acquisitions again using a Roper Scientific 1242 × 1152 cooled X-ray CCD detector. It was found that samples required 20−30 s at the set temperature (after the 2 min ramp) to equilibrate, so the first 150 s of data was generally not used for kinetic analysis. Kinetic effects were investigated by heating samples to multiple set temperatures.

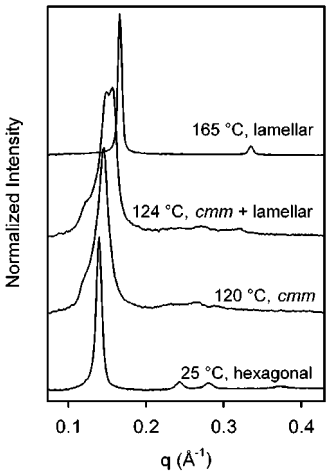

Figure 1. Sample of the observed phases obtained while heating a silica/surfactant composite at pH 11. For this heating run, the temperature was increased linearly at a rate of 4.40 °C/min. At low temperatures, hexagonal diffraction patterns such as the 25 °C pattern are observed. By 120 °C, the sample has transformed to a *cmm* structure. At 124 °C a mixture of *cmm* and lamellar is observed, and at higher temperatures clean lamellar patterns such as the 165 °C pattern are observed.

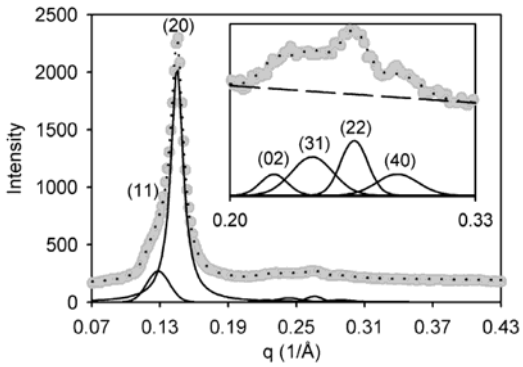

Figure 2. Rectangular phase composite at 120 °C as the sample was heated at 4.40 °C/min. Solid gray circles represent raw data, solid lines show peaks confined to a *cmm* symmetry fit to the data, and the dotted line is the sum of the peaks. Peaks are labeled on the graph in parentheses. Inset: Expansion of higher order peak region. The dashed line is the baseline.

Results

As shown in Figure 1, hexagonal silica/surfactant composites made with a 20 carbon alkyltrimethylammonium surfactant undergo a phase transition to a layered lamellar phase via a centered rectangular intermediate if treated in a pH 11 buffer. For these data, the temperature was increased at a rate of 4.40 °C. When pure water is used as the hydrothermal liquid, a similar hexagonal-to-lamellar transformation occurs, but no intermediates are detected. Figure 2 shows an enlargement of the 120 °C rectangular phase diffraction pattern from Figure 1. The four highest angle peaks shown were fit together with relationships between their positions defined by centered rectangular symmetry. Good quality fits were obtained, and the positions of the two lowest angle peaks were accurately predicted by the rectangular lattice constants determined from the four highest angle peaks.

In addition to proving that a centered rectangular intermediate exists, fitting all the peaks together gives information on the distortion of the lattice from hexagonal symmetry. As seen in Figure 3, a hexagonal lattice can be redefined as a rectangular lattice with the ratio of the a and b lattice vectors given by $a/b = \sqrt{3}$. For a/b ratios

(20) Tolbert, S. H.; Landry, C. C.; Stucky, G. D.; Chmelka, B. F.; Norby, P.; Hanson, J.; Monnier, A. *Chem. Mater.*, submitted.
(21) Landry, C. C.; Tolbert, S. H.; Gallis, K. W.; Monnier, A.; Stucky, G. D.; Norby, P.; Hanson, J. *Chem. Mater.*, in press.
(22) Burgoyne, J.; Holmes, M. C.; Tiddy, G. J. T. *J. Phys. Chem.* **1995**, *99*, 6054.
(23) Menger, F. H.; Littau, C. A. *J. Am. Chem. Soc.* **1993**, *115*, 10883.
(24) Norby, P. *J. Am. Chem. Soc.* **1997**, *119*, 5215. Norby, P.; Hanson, J. C. *Catal. Today* **1998**, *39*, 301.

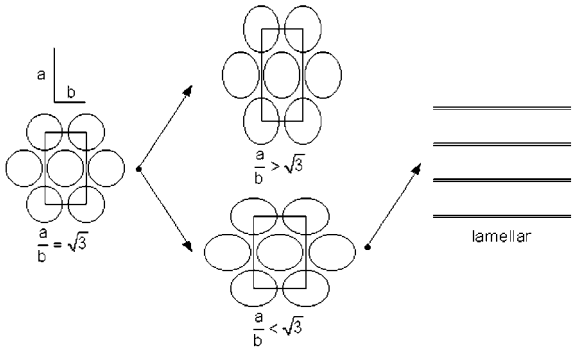

Figure 3. Possible deformations of the hexagonal lattice leading to centered rectangular morphologies. Only the distortion of $a/b < 1.73$ is in a direction that will form a lamellar structure.

other than $\sqrt{3}$, a hexagonal lattice cannot be used, and so centered rectangular symmetry is employed to express the crystal structure. Figure 3 illustrates the possible ways the hexagonal lattice may distort.[13] The four highest angle peaks in Figure 2 can be fit when the distortion is defined by either $a/b = 1.55$ or 1.97.

To distinguish the true lattice distortion, the two lowest angle peak positions may be predicted from the lattice spacing and distortion determined from the higher angle peaks. All nonisothermal runs were combined to increase the reliability of comparisons. The distortion of $a/b = 1.55$ has an rms fit error of 0.8 $mÅ^{-1}$ when predicting the two lowest angle peak positions. The distortion of $a/b = 1.97$, however, has an rms fit error of 1.8 $mÅ^{-1}$ when predicting the two lowest angle peak positions. While both of these fit errors are very small, they are still significant. In the low angle regime of this experiment, peak positions range between 125 and 160.0 $mÅ^{-1}$ and are significant to the 0.1 $mÅ^{-1}$ level. The source of the difference in fit error is the splitting of the lowest angle peaks predicted by each distortion. While both $a/b = 1.55$ and 1.97 reasonably predicted the position of the second peak shown in Figure 2 ($q \approx 145$ $mÅ^{-1}$), only $a/b = 1.55$ correctly predicted the lowest angle peak ($q \approx 130$ $mÅ^{-1}$). Because of the greater overall agreement in peak positions, we conclude that the hexagonal unit cell elongates along the rectangular *b* axis to produce an intermediate with an *a*/*b* ratio of 1.55 (Figure 3, bottom path).

Since a rectangular lattice can define both hexagonal and centered rectangular structures, it is possible to study how the material changes across the hexagonal-to-rectangular phase transition. By multiplying the *a* and *b* lattice vectors for each data frame, the change in unit cell area with temperature can be measured. Unit cell area is used because both phases are intrinsically two-dimensional; thus, lattice volumes are not measured in a diffraction experiment. It is assumed that the pores do not change significantly along the *c*-axis during the hydrothermal process and therefore changes in unit cell area can be related to changes in unit cell volume. Figure 4 shows the unit cell area as the composite is heated until it has halfway transformed to the lamellar phase. It can be seen that there is a large expansion of the unit cell area as the hydrothermal mixture is heated, followed by a steep drop in area as the material becomes rectangular. In regions where hexagonal/rectangular phase coexistence is present, the unit cell area shown in Figure 4 is the population weighted average unit cell area of each phase.

Besides tracking unit cell area, the phases present also provide information about how a phase transition progresses. Figure 5 shows changes in peak areas, which are proportional to the population of a phase, as the

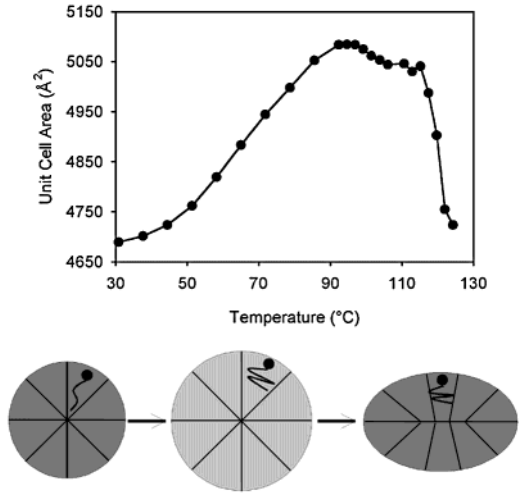

Figure 4. (Top) Rectangular unit cell area of a composite heated at 4.40 °C/min in a pH 11 buffer. A rectangular unit cell can be defined for hexagonal phase material by requiring a length-to-width ratio of 1.73. (Bottom) Diagram illustrating changes in the surfactant domains. The unit cell area initially expands, a phenomenon that could be driven either by volume increase or curvature reduction. The unit cell area begins to decrease, however, as the material transforms to the lower curvature rectangular phase at 95 °C. When the composite is halfway transformed to the lamellar phase at 124 °C, the unit cell area has greatly decreased, thus suggesting that a curvature decrease, not a unit cell volume increase, drives this transformation.

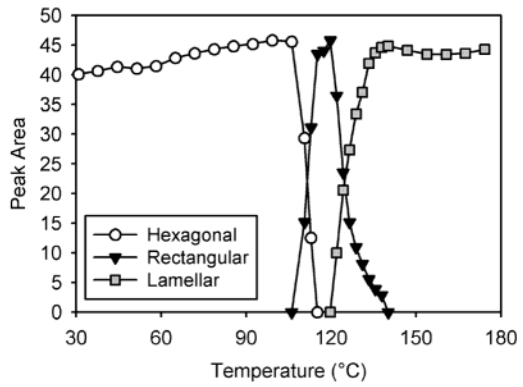

Figure 5. $(100)_{hexagonal}$, $(11)_{rectangular} + (20)_{rectangular}$, and $(100)_{lamellar}$ peak areas for a composite heated in a pH 11 buffer at 4.40 °C/min. The legend is on the graph. A simple progression of hexagonal-to-rectangular and then rectangular-to-lamellar transformations is observed because the rearrangements follow the lowest energy pathway.

material is heated on a linear temperature ramp. The hexagonal phase area is unchanged until 108 °C, at which point it falls as the rectangular phase grows in. The lamellar phase does not begin to form until the hexagonal phase is completely gone. As the lamellar phase grows in, the rectangular phase disappears. In Figure 6, this same type of simple phase progression is seen for a sample heated under isothermal conditions at 102 °C. The hexagonal phase completely transforms to rectangular; then an induction time occurs where there is no change, followed by a transformation from the rectangular phase to the lamellar structure. When the hydrothermal mixture is held at the higher temperature of 119 °C, however, a very different phase progression is observed (see Figure 7). The hexagonal phase now appears to have two different transformation pathways, transforming from hexagonal-to-rectangular-to-lamellar and also directly from hexagonal-to-lamellar. Different thermal conditions reveal that

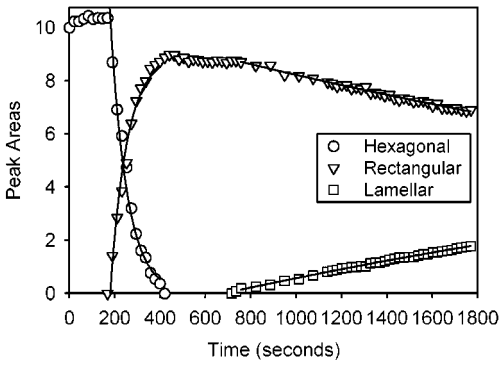

Figure 6. $(100)_{hexagonal}$, $(11)_{rectangular} + (20)_{rectangular}$, and $(100)_{lamellar}$ peak areas for a composite heated in a pH 11 buffer at 102 °C/min. The legend is on the graph. Black lines show global fits to peak areas for both transformations. A simple progression of hexagonal-to-rectangular and then rectangular-to-lamellar transformations is observed because the rearrangements follow the lowest energy pathway.

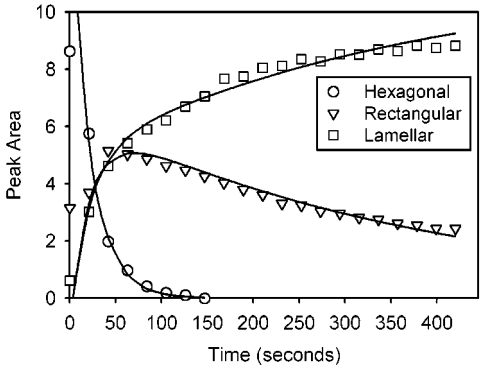

Figure 7. $(100)_{hexagonal}$, $(11)_{rectangular} + (20)_{rectangular}$, and $(100)_{lamellar}$ peak areas for a composite heated in a pH 11 buffer at 119 °C/min. The legend is on the graph. Black lines show global fits to peak areas for both transformations. A complex progression of phases is observed as hexagonal-to-rectangular-to-lamellar and direct hexagonal-to-lamellar transformations occur simultaneously. Overdriving this transformation using a high holding temperature makes it possible to access higher energy pathways. The first point for each phase does not lie on the fit lines because the material is not thermally equilibrated until 21 s into the run.

multiple energy dependent pathways exist for the hexagonal-to-lamellar transformation.

Discussion

We first need to understand the chemical processes that allow for the formation of an intermediate phase. Then we will explore the effect of the chemical changes on surfactant packing, discuss the energetics of the observed transformations, and finally investigate the forces that drive this transformation. The silica chemistry that occurs during heating is a theme that will unite all of these phenomena.

Significant changes in silica chemistry between experiments performed in water[3] and experiments performed in this work are the result of the pH 11 buffer used as the hydrothermal medium. Increased hydroxide concentration in the solution will modify the polymerization and charge density of the silica walls when heated under hydrothermal conditions. Polymerization, in turn, will change the amount of surfactant in the composite and alters the composite's framework strength, all of which affect phase stability. Each surfactant molecule in the pores is electrostatically bound to a $Si-O^-$ group on the pore wall.[25] Silica polymerization should result in condensation of $Si-O^-$ species and the liberation of OH^- groups, thus forcing surfactant into solution.[26] At higher pH, net silica condensation is slower, and as a result, less surfactant should be expelled.[26] Thus, the large amount of surfactants retained in each pore should be packed more tightly than if the material had been heated in water. When composites are heated in water, thermal motion increases the effective volume of the surfactant tails, resulting in a driving force to distort the framework in order to accommodate the greater tail volume.[27,28] In high pH solutions where surfactant loss should be minimized, this driving force for rearrangement should be larger than that for experiments performed in water. As suggested by phase stability in liquid crystalline systems, one way to accommodate this increased tail volume is by distortion to a rectangular structure. In surfactant/water liquid crystals, distortions are also made possible by counterion screening of surfactant head-to-head repulsions.[8,9] In our composites, the high pH used maintains a high silica charge that may screen surfactant head-to-head repulsion and allow more surfactants to be associated with the framework. Thus, a combination of surfactant packing effects and increased electrostatic shielding probably encourages the formation of the intermediate phase found in this work.

The less polymerized framework found in these experiments might also lower kinetic barriers and allow for a wider range of phases to form. It has been shown that during heating under hydrothermal conditions in water, the silica framework will condense and raise the activation barrier for transformation.[3] Under the high pH conditions found in this work, however, silica condensation is much less likely to occur,[4] and so a lower activation barrier will be present, allowing the less interbonded silica framework to more facilely distort. The *cmm* phase is thus favored as a stable intermediate based on both kinetic and energetic arguments.

Now that the appearance of the *cmm* phase is understood, we can use the intermediate to learn more about the transformation mechanism. The distortion of the centered rectangular phase is experimentally determined to be $a/b = 1.55$. Previous experiments studying the hexagonal-to-lamellar transformation in water have shown that the transition propagates from one adjacent pore to another unidirectionally across the material.[3] This result is found by analyzing the kinetics of the transformation and is consistent with the elongation of the hexagonal unit cell given by $a/b = 1.55$. The value 1.55 corresponds to expansion in the direction of the hexagonal-to-lamellar transformation and shrinking perpendicular to it. The shrinkage of the hexagonal layers ($a/2$ in Figure 3) is also consistent with the observation that the fundamental repeat distance in the final lamellar phase is smaller than this same repeat distance in the starting hexagonal structure. Therefore, a rectangular intermediate with $a/b = 1.55$ is halfway between the starting and ending structures along a transition path that is defined by a one-dimensionally propagating distortion. As a result, the rectangular elongation nicely confirms the previously determined one-dimensional transformation mechanism.[3]

(25) Monnier, A.; Schuth, F.; Huo, Q.; Kumar, D.; Margolese, D.; Maxwell, R. S.; Stucky, G. D.; Krishnamurty, M.; Petroff, P.; Firouzi, A.; Janicke, M.; Chmelka, B. F. *Science* **1993**, *261*, 1299.

(26) Gross, A. F.; Le, V. H.; Kirsch, B. L.; Riley, A. E.; Tolbert, S. H. *Chem. Mater.*, submitted.

(27) Wood, R. M.; McDonald, M. P. *J. Chem. Soc., Faraday Trans. 1* **1985,** *81*, 273.

(28) Kekicheff, P.; Cabane, B. *J. Phys.* **1987**, *48*, 1571.

Scheme 1

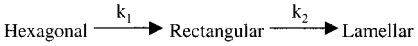

The energetics of transformation can be better understood by examining the kinetic barriers involved in the process. To do this, we first need to understand the range of possible transition mechanisms. We can then use transition points and rate constants to calculate activation energies. Figures 5−7 emphasize the range of transformation pathways available for getting from the hexagonal to the lamellar structure. A linear temperature ramp (Figure 5) accesses only the kinetically lowest energy pathway. A linear progression of phases is observed as the material is driven stepwise through the available phases (Scheme 1). This behavior occurs because the incrementally increasing temperature allows only enough energy to get to the next phase. No extra energy is available to access higher energy paths. A low temperature isothermal experiment (Figure 6), like the linear ramp, also accesses only a linear progression of phases (Scheme 1). This is because again the system has only enough energy to transform along the lowest energy path.

The low temperature isothermal data are fit to a model that describes a linear progression of phases. The fraction of material transformed is followed as a function of time to determine a rate constant using the Avrami rate law.[29]

$$\ln(1 - \alpha) = (kt)^n$$

Here α is the fraction transformed, k is the rate of the transformation, t is the time, and n is the dimensionality of the phase transition. This equation has been found to describe a wide range of solid−solid phase transformations. The hexagonal-to-lamellar transformation in silica/surfactant composites has been shown to transform with $n = 1$, and so we will use this value for the related rectangular-to-lamellar transition studies here.[3,30]

The hexagonal-to-rectangular transformation has rate k_1, and the rectangular-to-lamellar transformation has rate k_2 (Scheme 1). An example of fitting to this model is seen in the black lines in Figure 6. The high fit quality suggests that we have chosen the right transition mechanism. The long induction time (where nothing occurs) between the phase transformations clearly demonstrates the sequential nature of the phase progression and allows us to determine k_1 and k_2 independently using the Avrami equation.

Figure 7 shows a more complex situation. At the higher holding temperature of 119 °C, more energy is available to the system. At this temperature no induction times exist, and both the lowest energy hexagonal-to-rectangular-to-lamellar transformation and the higher energy direct hexagonal-to-lamellar transformation are observed. This is seen quantitatively in the data—both the rectangular and lamellar peak areas rise together. The complex phase coexistence results from excess thermal energy. The progression of phases is supported by data analysis: All isothermal data may be successfully fit to a model that has three possible transformations, each with its own rate (Scheme 2). The hexagonal-to-rectangular transformation has rate k_1, the rectangular-to-lamellar transformation has rate k_2, and the direct hexagonal-to-lamellar transformation now has rate k_3. The derivation of an integrated rate law for this model based on the Avrami equation is shown in the Appendix. Data from all phases are fit simultaneously in a global fit, which is advantageous because k_1, k_2, and k_3 are determined together and used to determine both the amplitude and the rate of change of each phase. The black lines in Figure 7 show the global fit to the model described above, which successfully describes the behavior of the data. In addition, the model gives rectangular-to-lamellar rates (k_2) that correlate well with the data obtained at low temperature using the simpler Scheme 1. Data fit with both mechanisms were used in the Arrhenius plot (Figure 8, bottom), showing that the proposed transformation mechanisms are consistent with all of the data.

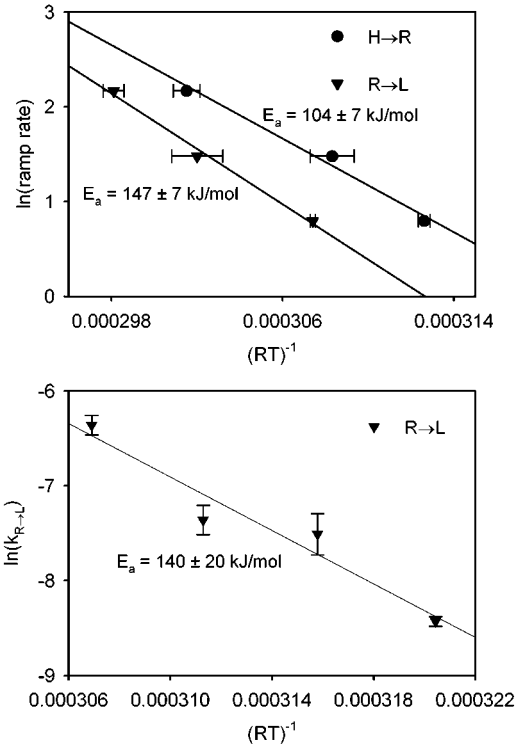

Figure 8. (Top) Nonisothermal averaged data fit to the Ozawa equation for the hexagonal-to-rectangular and rectangular-to-lamellar transformations. The steeper slope for the rectangular-to-lamellar data indicates that this process has a higher activation energy. (Bottom) Averaged isothermal data are fit to the Arrhenius equation for the rectangular-to-lamellar transformation ($k_{R\to L} = k_2$). Numerical values for E_a and legends are shown on both graphs.

Scheme 2

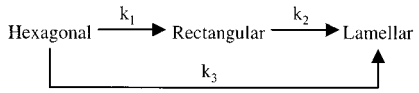

Table 1

T (°C)	k_3/k_1
119	1.2
113	0.8
108	0.2
102	0

The higher energy hexagonal-to-lamellar pathway can be seen to shut down when less excess energy is present. Table 1 shows that the rate of the hexagonal-to-lamellar pathway decreases relative to the rate of the hexagonal-to-rectangular pathway with decreasing temperature. Note that data are averaged over all runs performed at each temperature. Only one run at 108 °C clearly shows $k_3 \neq 0$, so k_3/k_1 represents only that particular run.

(29) Avrami, M. *J. Chem. Phys.* **1939**, *7*, 1102. Avrami, M. *J. Chem. Phys.* **1940**, *8*, 212. Avrami, M. *J. Chem. Phys.* **1941**, *9*, 177.
(30) Ozawa, T. *Bull. Chem. Soc. Jpn.* **1965**, *38*, 1881.

Table 2.

	hexagonal to *cmm*	*cmm* to lamellar	hexagonal to lamellar
Ozawa (nonisothermal)	104 ± 7 kJ/mol	147 ± 7 kJ/mol	does not occur
Arrhenius (isothermal)	not determined	140 ± 20 kJ/mol	>200 kJ/mol

The bifurcation of pathways in these experiments shows that in hydrothermal synthesis multiple transformation pathways may be available. In these experiments, all pathways lead to the same final phase, but in other systems, the pathways may end in different final products.[12,20,21] Understanding that driving force and temperature directly affect the accessible phases should help in understanding and possibly predicting phase transformations in other inorganic/surfactant composite materials.

To calculate activation energies, we use established methods. It has been shown that it is possible to relate the midpoints of phase transitions measured while heating at different linear ramp rates to the activation energy for transformation.[30] Ozawa expressed the relationship as

$$\ln(b) = -\frac{E_a}{RT} + \text{int}$$

where b is the ramp rate, E_a is the activation energy, R is the gas constant, T is the absolute transition temperature, and int is the intercept of the plot (which is not important for determining the activation energy). We use the Ozawa equation because it describes many phase change processes well and because it has been shown to produce reasonable agreement with both isothermal[30] and other nonisothermal methods.[31] Each experimental nonisothermal run gives a (b,T) point; multiple runs with different ramp rates on the same sample are used to calculate the activation energy for transformation.

Figure 8 (top) shows Ozawa fit lines for averaged data from samples heated at 8.8, 4.4, and 2.2 °C/min. The steeper slope of the line from the rectangular-to-lamellar transition points indicates a higher activation energy. Numerically, these slopes correspond to hexagonal-to-rectangular and rectangular-to-lamellar transformation activation energies of 104 ± 7 and 147 ± 7 kJ/mol, respectively.

The accuracy of the activation energies determined using nonisothermal methods is supported by an activation energy determined using isothermal methods. Using the rate constants (k) described above, we can calculate activation energies by fitting the (T,k) points using the Arrhenius equation:

$$\ln k = -\frac{E_a}{RT} + \text{int}$$

Here k is the rate constant, R is the gas constant, T is the absolute temperature, E_a is the activation energy, and int is the intercept of the line. Figure 8 (bottom) shows an Arrhenius plot for the rectangular-to-lamellar transition (k_2 data). An activation energy of 140 ± 20 kJ/mol is found, in excellent agreement with the nonisothermal result. The hexagonal-to-rectangular activation energy cannot be accurately determined from the k_1 isothermal data due to the rapid rate of this transformation and our limited ability to jump the temperature. When samples are held at higher isothermal temperatures, the direct hexagonal-to-lamellar transformation is seen in addition to the usual hexagonal-to-rectangular-to-lamellar transition. Observation of the hexagonal-to-lamellar transformation is hindered by the same problems as those for the hexagonal-to-rectangular change, but we can estimate that the activation energy for this phase change is in excess of 200 kJ/mol from the temperature dependent k_3 data. A summary of all activation energies is shown in Table 2.

The activation energies should correlate with the progression of observed phases. By simple kinetic arguments, the transformation with the lowest activation energy should occur first in a kinetically limited transformation scheme. This is demonstrated in our data: At low temperatures, the hexagonal phase transforms first to the rectangular phase (E_a = 104 ± 7 kJ/mol) rather than directly becoming lamellar (E_a > 200 kJ/mol). Perhaps more importantly, to produce a kinetically stable intermediate, the activation energy for formation of the intermediate must be smaller than the activation energy for the subsequent reaction of the intermediate to form products. In our experiments, the hexagonal-to-rectangular activation energy (E_a = 104 ± 7 kJ/mol) is, in fact, lower than the rectangular-to-lamellar activation energy (E_a = 140−147 ± 20 kJ/mol), predicting a stable intermediate phase, as is experimentally observed.

An intermediate forms only when composites are treated at pH 11 and not in pure water. On the basis of the ideas presented above, a possible explanation for this phenomenon can be hypothesized on the basis of kinetics. If the rectangular-to-lamellar activation energy is lower than the hexagonal-to-rectangular activation energy, then the intermediate would not be stable at the transition temperature, and the material would immediately become lamellar. A stable intermediate could occur if increased hydrolysis (or more likely, decreased condensation) lowered the hexagonal-to-rectangular activation energy more than the rectangular-to-lamellar activation energy. A more rapid drop in the hexagonal-to-rectangular activation energy is reasonable because fewer bonds should need to be broken to distort the structure (hexagonal → *cmm*) than to break all the connections between the hexagonal cylinders (*cmm* → lamellar). A less condensed, more flexible, framework might be able to accommodate the hexagonal-to-rectangular transition with minimal energy increase. The transition to the lamellar phase necessitates the breaking of Si−O−Si bonds and is, therefore, a high-energy process at any pH.

The energetics for this transformation make sense with the data, but the driving force for this phase change still needs to be examined. Information about the driving force can be found by looking at the unit cell area shown in Figure 4. The unit cell area initially expands in response to the thermal motion of the surfactant tails but then rapidly decreases during the phase transition to the rectangular phase. By examining the forces that drive analogous liquid crystal phase transformations (volume expansion and curvature), we will determine the driving force for the formation of the rectangular and lamellar phases. A diagram of these changes is shown in Figure 4 (bottom). Volume expansion should have the largest effect on the hexagonal and rectangular phases because, unlike the lamellar phase, *cmm* and hexagonal phases have confined volumes. If volume expansion is important, the material should expand its unit cell volume throughout

(31) Tiernan, M. J.; Barnes, P. A.; Parkes, G. M. B. *J. Phys. Chem. B* **1999**, *103*, 6944.

the hexagonal and rectangular stability regions. This is not observed.

Thermal motion of the surfactant tails should also increase the tail width and decrease the tail length, resulting in a decrease in surfactant curvature. For the phases observed here, hexagonal has the highest curvature, rectangular has medium curvature, and lamellar is the lowest curvature phase.[10,27] A hexagonal structure with a large unit cell area also has a lower radius of curvature than a hexagonal structure with a small unit cell area. A lowering of curvature throughout the transformation is thus observed as the hexagonal unit cell expands and then transforms to the lower curvature rectangular phase, and finally the zero curvature lamellar phase. However, unit cell area is not gained throughout the hexagonal-to-rectangular transformation, as shown in Figure 4 from 119 to 124 °C. This result suggests that volume expansion is not the primary driving force for transformation and that a change in curvature is the main cause of phase transformations in these composite materials.

Conclusions

A *cmm* centered rectangular intermediate phase has been observed during a hexagonal-to-lamellar phase transition. The appearance of this intermediate seems to depend strongly on the hydrothermal processing conditions. Only under basic conditions, where little silica condensation occurs and minimal surfactant is lost, is it possible to find this centered rectangular intermediate. The new symmetry of the intermediate allows us to learn about both the mechanism of transformation and the driving force for rearrangement. The rectangular distortion confirms the one-dimensional transformation mechanism predicted from kinetic arguments and allows us to show that changes in surfactant curvature, rather than volume expansion, are the primary driving force for transformations. The activation energy measured for the hexagonal-to-rectangular transition using nonisothermal methods is 104 ± 7 kJ/mol. The rectangular-to-lamellar activation energy is 147 ± 7 kJ/mol and 140 ± 20 kJ/mol, determined using nonisothermal and isothermal methods, respectively. The relative heights of these energy barriers correspond well to the order of the observed phases and to the stability of the intermediate phase.

This work shows that accessible phases are very sensitive to silica condensation. By producing a rectangular phase, we have demonstrated that phase control of these materials through silica chemistry is possible. In addition, now that the importance of changes in surfactant curvature in driving phase transitions has been demonstrated, it may be possible to design surfactants to exploit this effect during hydrothermal processing. Perhaps most important from a practically point of view, however, the results emphasize the fact that, in silica/surfactant composite synthesis, postsynthesis silica chemistry and the details of the temperature profile should be explored as reaction parameters to realize the full range of possible kinetically controlled end products.

Acknowledgment. The authors thank B. J. Schwartz and E. R. Barthel for helpful discussions on the analysis of kinetic data. Help with real time data collection from A. E. Riley is gratefully acknowledged. Data in this work were collected at the Stanford Synchrotron Radiation Laboratory (SSRL), which is operated by the Department of Energy, Office of Basic Energy Sciences. This work was supported by the National Science Foundation under Grant DMR-9807190.

Appendix

The first step in deriving kinetic equations for the change in population of the hexagonal, rectangular, and lamellar phases is to write down a differential rate law for each transition. All k's refer to Scheme 2.

$$\frac{dH}{dt} = -k_1 H - k_3 H \tag{A.1}$$

$$\frac{dR}{dt} = k_1 H - k_2 R \tag{A.2}$$

$$\frac{dL}{dt} = k_2 R + k_3 H \tag{A.3}$$

H, R, and L are the hexagonal, rectangular, and lamellar phase populations, respectively. t is time. k_1, k_2, and k_3 are the hexagonal-to-rectangular, the rectangular-to-lamellar, and the hexagonal-to-lamellar transformation rates, respectively. Using these equations, a matrix can be constructed that will describe all changes in the sample.

$$\frac{d}{dt}\begin{bmatrix} H \\ R \\ L \end{bmatrix} = \begin{bmatrix} -k_1 - k_3 & 0 & 0 \\ k_1 & -k_2 & 0 \\ k_3 & k_2 & 0 \end{bmatrix}\begin{bmatrix} H(t) \\ R(t) \\ L(t) \end{bmatrix} \tag{A.4}$$

We take the determinate of this matrix and find its eigenvalues, which are 0, $-k_2$, and $-k_1 - k_3$. The eigenvalues are used to find the eigenvectors, and we construct the solutions to differential equations A.1−A.3.

$$\begin{bmatrix} H(t) \\ R(t) \\ L(t) \end{bmatrix} = c_1\begin{bmatrix} 1 \\ \dfrac{-k_1}{k_1 - k_2 + k_3} \\ \dfrac{-k_3}{k_1 + k_3} + \dfrac{k_1 k_2}{(k_1 + k_3)(k_1 - k_2 + k_3)} \end{bmatrix} e^{-(k_1 + k_3)t} + c_2\begin{bmatrix} 0 \\ 1 \\ -1 \end{bmatrix} e^{-(k_2)t} + c_3\begin{bmatrix} 0 \\ 0 \\ 1 \end{bmatrix} \tag{A.5}$$

where c_1, c_2, and c_3 are the undefined constants of the eigenvectors. The maximum population of each phase is normalized to 1. We apply boundary conditions based on this normalization to solve for c_1, c_2, and c_3: $H(0) = 1$, $R(0) = 0$, $L(\infty) = 1$. Using these boundary conditions, we find that the eigenvector constants are

$$c_1 = 1 \tag{A.6}$$

$$c_2 = \frac{k_1}{k_1 - k_2 + k_3} \tag{A.7}$$

$$c_3 = 1 \tag{A.8}$$

All time dependent population changes in each sample are thus fit concurrently with the following three equations

in order to find the rate constants k_1, k_2, and k_3.

$$H(t) = e^{-(k_1+k_3)t} \quad \text{(A.9)}$$

$$R(t) = \frac{-k_1}{k_1 - k_2 + k_3}(e^{-(k_1+k_3)t} - e^{-(k_2)t}) \quad \text{(A.10)}$$

$$L(t) = \left(\frac{-k_3}{k_1 + k_3} + \frac{k_1 k_2}{(k_1 + k_3)(k_1 - k_2 + k_3)}\right)e^{-(k_1+k_3)t} - \frac{k_1}{k_1 - k_2 + k_3}e^{-(k_2)t} + 1 \quad \text{(A.11)}$$

LA0018080